

Tensor-force effects on shell-structure evolution in $N = 82$ isotones and $Z = 50$ isotopes in the relativistic Hartree-Fock theory

Zhiheng Wang (王之恒),^{1,2} Tomoya Naito (内藤智也),^{3,4} and Haozhao Liang (梁豪兆)^{3,4}

¹*School of Nuclear Science and Technology, Lanzhou University, Lanzhou 730000, China*

²*Joint department for nuclear physics, Lanzhou University and Institute of Modern Physics, Chinese Academy of Sciences, Lanzhou 730000, China*

³*Department of Physics, Graduate School of Science, The University of Tokyo, Tokyo 113-0033, Japan*

⁴*RIKEN Nishina Center, Wako 351-0198, Japan*

(Dated: March 20, 2022)

The evolution of the energy difference between the neutron states $1i_{13/2}$ and $1h_{9/2}$ in the $N = 82$ isotones and that between the proton states $1h_{11/2}$ and $1g_{7/2}$ in the $Z = 50$ isotopes are investigated within the framework of the relativistic Hartree-Fock theory, using the density-dependent effective interactions PKA1 and PKO1 ($i = 1, 2, 3$). By identifying the contributions of the tensor force, which is naturally induced via the Fock terms, we find that the tensor force plays crucial roles in the evolution of the shell structure. The strength of the tensor force is also explored. It is found that moderately increasing the coupling strength of pion-nucleon coupling, i.e., f_π , will significantly improve the description of the shell-structure evolution. In particular, reducing the density dependence of f_π is shown to be more preferable, in comparison to enlarging f_π with a factor. This is in consistence with the idea of “tensor renormalization persistency” and provides valuable guidance for the development of nuclear energy density functional in the relativistic framework.

I. INTRODUCTION

Shell structure belongs to the most important properties of nuclear systems. By introducing strong spin-orbit coupling to the harmonic oscillator potential, Haxel, Jensen, and Suess [1] and Mayer [2] successfully explained the magic numbers associated with the shell closure. Owing to the development of modern radioactive nuclear beam facilities and experimental detectors [3–10], the landscape of nuclei extends from the β -stable line to the regime of exotic ones with unbalanced N/Z ratio [11, 12]. Meanwhile, traditional shell structure does not remain solid. The modification of shell closures has become one of the most intriguing issues in the recent decades [13, 14].

The shell evolution, which leads to the appearance of the new magic numbers as well as the disappearance of the traditional ones, challenges the traditional understanding of nuclear physics [15–17]. For example, the tensor force [18, 19], which had been neglected for a long time in the effective interactions [20], has regained tremendous concerns, mainly because of its characteristic effects on the spin-orbit splitting and hence on the shell evolution [21]. It has been pointed out that the tensor force is repulsive between the two nucleons which are both spin-up ($j = l + 1/2$) or spin-down ($j = l - 1/2$), while attractive when one nucleon is spin-up and the other is spin-down [21]. Such a character of spin dependence affects the spin-orbit splitting, especially for the nuclides located in the exotic regime.

During the last two decades, the tensor-force effects on the single-particle energies have been studied extensively, in both the nuclear density functional theory (DFT) [22–39] and the shell model [15, 21, 40–44].

In spite of this, the strength of the in-medium effec-

tive tensor force and even its sign are still under discussion [14, 34]. Traditionally, the parameters of the effective interactions are fitted to the bulk properties, which are shown to be not sensitive enough to the tensor force. As a result, the properties of the in-medium effective tensor force are far way from being efficiently constrained. Actually, to pin down the nature of the tensor force is one of the crucial aspects for the ultimate understanding of the effective nuclear interactions employed in, for example, the DFT [23, 37, 45–49]. To achieve this, one needs to find the observables that are sensitive to the tensor force but not so much to the other components of nuclear force. The single-particle energies, which are largely affected by the spin-orbit splitting, can serve as such kind of benchmarks. It is thus of great significance to study how the tensor force affects the single-particle energies, especially the shell-structure evolution along the isotopic or isotonic chains.

In 2004, by neutron and proton transfer reactions, Schiffer *et al.* [50] investigated the differences between the energies of the neutron (ν) states $1i_{13/2}$ and $1g_{9/2}$ in the $N = 82$ isotones and those of the proton (π) states $1h_{11/2}$ and $1g_{7/2}$ in the $Z = 50$ isotopes. This experimental progress immediately attracted a lot of interests in the theoretical researches and became a popular playground for investigating the shell evolution and the hidden mechanisms. In particular, Colò *et al.* [51] found that the introduction of tensor force on top of the Skyrme effective interactions can fairly well reproduce the isospin dependence of the energy differences in the above-mentioned isotones and isotopes, while the effective interactions without explicit tensor force fail. The tensor-force effects were also explored within the relativistic framework, i.e., the relativistic Hartree-Fock (RHF) theory [26]. It was found that the tensor force

arising from the pion exchange plays a crucial role in explaining the evolution of the energy difference with the neutron or proton number.

The tensor force can be added on top of the existing Skyrme interactions perturbatively and refitted individually; the SLy5 + T [51] and SIII + T [24] were established in this way. An alternative way, which is practically more accurate and more systematic, is to fit the tensor force on the same footing with the central terms, and the representative functionals are the Skxta and Skxtb [40], *TIJ* family [25], SkP_T, SLy4_T, and SkO_T [52], and SAMi-T [37]. Similar strategies to introduce the tensor force have also been applied for the finite-range Gogny interactions [23, 40]. Nevertheless, both of these two ways inevitably increase the number of free parameters due to the additional inclusion of the tensor force, which may be one of the reasons why the tensor force is neglected in most of the effective interactions in the nonrelativistic framework.

In the covariant density functional theory (CDFT) with the exchange terms, namely the RHF theory, not only the strong spin-orbit coupling can be treated naturally, but also the tensor force is consistently contained via the Fock term of the relevant meson-nucleon interactions, without extra free parameters [53–57]. On the other hand, the tensor force is mixed together with the other components, e.g., the spin-orbit force and other central forces. This leads to great difficulties in the quantitative analysis of the tensor force in CDFT, despite the noticeable progress on the tensor-force effects arising from the π -pseudovector and ρ -tensor couplings [26, 58–62]. In particular, a set of formula with Lorentz covariance were developed to describe the spin-dependent nature of the nuclear force within the RHF theory in 2015, and they could reproduce the spin dependence of the two-body interaction matrix elements quite well [63–65]. However, these formulas are not straightforwardly related to the tensor force in the conventional sense. Thus, the corresponding results cannot be compared directly with the tensor-force effects calculated by the nonrelativistic DFT. Aiming at a direct comparison between the tensor-force effects in the CDFT and those in the nonrelativistic DFT, recently, the tensor force in each meson-nucleon coupling has been identified within the RHF theory [66]. In addition, a method to quantitatively evaluate the contributions of the tensor force arising from these meson-nucleon couplings has also been illustrated.

In this work, we will investigate the isospin evolution of the single-particle energy differences in the $N = 82$ isotopes and the $Z = 50$ isotopes mentioned above within the RHF theory. In particular, the effects of the tensor force will be studied with the method newly developed in Ref. [66]. The strength of the tensor force will be explored, aiming to provide guidance for the future development of the effective interactions. To this end, it is noticed that the single-particle energies, as well as the collective excitations, are affected by various “dynamic correlations”, among which the particle-vibration cou-

pling (PVC) [67–73] is considered to play the most important roles, especially for the spherical nuclei. Thus, the experimental data of the single-particle energy are not supposed to be compared directly with the corresponding results calculated by DFT which are purely mean-field-level quantities.

In Sec. II, we briefly introduce the framework of RHF theory, as well as the main ideas to extract the contributions of the tensor force in the RHF theory. The results will be discussed in Sec. III. A summary and perspectives will be given in Sec. IV.

II. THEORETICAL FRAMEWORK

In this section, the basic framework of the RHF theory will be recalled, and more details can be found in Refs. [53, 54, 74–81]. The method to extract the contributions of the tensor force will also be briefly presented.

A. Relativistic Hartree-Fock theory

In the relativistic framework, the nucleons interact with each other via the exchange of mesons and photons [20, 82–87]. Based on this picture, the starting point of the RHF theory is a standard Lagrangian density, which contains the degrees of freedom associated with the nucleon field, various meson fields, and the photon field. Through the Legendre transformation, the Hamiltonian of the system can be derived. With the equations of motion for the mesons and photons, the Hamiltonian can be expressed with only the degree of freedom of the nucleon field, which reads

$$H = \int d^3x \bar{\psi}(x) [-i\boldsymbol{\gamma} \cdot \boldsymbol{\nabla} + M] \psi(x) + \frac{1}{2} \sum_{\phi} \iint d^3x d^4y \bar{\psi}(x) \bar{\psi}(y) \Gamma_{\phi}(x, y) D_{\phi}(x, y) \times \psi(y) \psi(x), \quad (1)$$

where ϕ denotes the meson-nucleon couplings, including here the Lorentz σ -scalar (σ -S), ω -vector (ω -V), ρ -vector (ρ -V), ρ -tensor (ρ -T), ρ -vector-tensor (ρ -VT), and π -pseudovector (π -PV) couplings, as well as the photon-vector (A -V) coupling.

The interaction vertices $\Gamma_{\phi}(x, y)$ in the Hamiltonian (1) read

$$\Gamma_{\sigma\text{-S}}(x, y) = -[g_{\sigma}]_x [g_{\sigma}]_y, \quad (2a)$$

$$\Gamma_{\omega\text{-V}}(x, y) = +[g_{\omega}\gamma_{\mu}]_x [g_{\omega}\gamma^{\mu}]_y, \quad (2b)$$

$$\Gamma_{\rho\text{-V}}(x, y) = +[g_{\rho}\gamma_{\mu}\vec{\tau}]_x \cdot [g_{\rho}\gamma^{\mu}\vec{\tau}]_y, \quad (2c)$$

$$\Gamma_{\rho\text{-T}}(x, y) = + \left[\frac{f_{\rho}}{2M} \sigma_{\mu\nu} \vec{\tau} \partial^{\nu} \right]_x \cdot \left[\frac{f_{\rho}}{2M} \sigma^{\mu\lambda} \vec{\tau} \partial_{\lambda} \right]_y, \quad (2d)$$

$$\Gamma_{\rho\text{-VT}}(x, y) = + \left[\frac{f_\rho}{2M} \sigma_{\mu\nu} \vec{\tau} \partial^\mu \right]_x \cdot [g_\rho \gamma^\nu \vec{\tau}]_y + (x \leftrightarrow y), \quad (2e)$$

$$\Gamma_{\pi\text{-PV}}(x, y) = - \left[\frac{f_\pi}{m_\pi} \vec{\tau} \gamma_5 \gamma_\mu \partial^\mu \right]_x \cdot \left[\frac{f_\pi}{m_\pi} \vec{\tau} \gamma_5 \gamma_\nu \partial^\nu \right]_y, \quad (2f)$$

$$\Gamma_{A\text{-V}}(x, y) = + \left[e \gamma_\mu \frac{1 - \tau_3}{2} \right]_x \left[e \gamma^\mu \frac{1 - \tau_3}{2} \right]_y, \quad (2g)$$

with the meson-nucleon coupling strengths g and f , the nucleon mass M , and the meson masses m . When the retardation effect is neglected [74], the meson and photon propagators, $D_\phi(x, y)$, become the standard Yukawa and Coulomb forms,

$$D_\phi(x, y) = \frac{1}{4\pi} \frac{e^{-m_\phi |\mathbf{r}_1 - \mathbf{r}_2|}}{|\mathbf{r}_1 - \mathbf{r}_2|}, \quad (3a)$$

$$D_{A\text{-V}}(x, y) = \frac{1}{4\pi} \frac{1}{|\mathbf{r}_1 - \mathbf{r}_2|}, \quad (3b)$$

respectively. Hereafter, we use \mathbf{r}_1 and \mathbf{r}_2 to denote the spatial coordinates at vertices x and y , and the indices “1” and “2” are always used to denote the vertices.

The meson-nucleon coupling strengths are taken as functions of the baryonic density. For the convenience of the following discussions about the strength of the tensor force, here we explicitly present the density dependence of the π -PV coupling f_π , which reads

$$f_\pi(\rho_b) = f_\pi(0) e^{-a_\pi \xi}, \quad (4)$$

where $\xi = \rho_b / \rho_{\text{sat}}$, ρ_{sat} denotes the saturation density of nuclear matter, and $f_\pi(0)$ corresponds to the coupling strength at zero density. The density dependence of the other meson-nucleon couplings can be referred to Refs. [53, 54].

The nucleon-field operators $\psi(x)$ and $\psi^\dagger(x)$ can be expanded on the set of creation and annihilation operators defined by a complete set of Dirac spinors $\{\varphi_\alpha(\mathbf{r})\}$. Then, the energy functional can be obtained through the expectation value of the Hamiltonian on the trial Hartree-Fock state under the no-sea approximation [82]. It can be expressed as

$$\begin{aligned} E &= \langle \Phi_0 | H | \Phi_0 \rangle - AM \\ &= E^K + \sum_\phi (E_\phi^D + E_\phi^E) \\ &= \sum_\alpha \int d\mathbf{r} \bar{\varphi}_\alpha(\mathbf{r}) (-i\boldsymbol{\gamma} \cdot \boldsymbol{\nabla} + M) \varphi_\alpha(\mathbf{r}) - AM \\ &\quad + \frac{1}{2} \sum_{\phi, \alpha\beta} \left\{ \iint d\mathbf{r}_1 d\mathbf{r}_2 \bar{\varphi}_\alpha(\mathbf{r}_1) \bar{\varphi}_\beta(\mathbf{r}_2) \Gamma_\phi(\mathbf{r}_1, \mathbf{r}_2) D_\phi(\mathbf{r}_1, \mathbf{r}_2) \varphi_\alpha(\mathbf{r}_1) \varphi_\beta(\mathbf{r}_2) \right. \\ &\quad \left. - \iint d\mathbf{r}_1 d\mathbf{r}_2 \bar{\varphi}_\alpha(\mathbf{r}_1) \bar{\varphi}_\beta(\mathbf{r}_2) \Gamma_\phi(\mathbf{r}_1, \mathbf{r}_2) D_\phi(\mathbf{r}_1, \mathbf{r}_2) \varphi_\beta(\mathbf{r}_1) \varphi_\alpha(\mathbf{r}_2) \right\}, \end{aligned} \quad (5)$$

where E^K denotes the kinetic energy, and E_ϕ^D and E_ϕ^E correspond to the energy contributions from the direct (Hartree) and exchange (Fock) terms, respectively.

In the spherically symmetric systems, the single-particle states, which are Dirac spinors here, can be specified by a set of quantum numbers $\alpha \equiv (a, m_\alpha) \equiv (\tau_a, n_a, l_a, j_a, m_\alpha)$. Explicitly, the Dirac spinors have the following expression,

$$\varphi_\alpha(\mathbf{r}) = \frac{1}{r} \begin{pmatrix} iG_a(r) \\ F_a(r) \hat{\boldsymbol{\sigma}} \cdot \hat{\mathbf{r}} \end{pmatrix} \mathcal{Y}_\alpha(\hat{\mathbf{r}}) \chi_{\frac{1}{2}}(\tau_a), \quad (6)$$

where $\mathcal{Y}_\alpha(\hat{\mathbf{r}})$ are the tensor spherical harmonics defined through the coupling of the spherical harmonics and the spin spinors [88].

The variation of the energy functional with respect to the Dirac spinors leads to the Hartree-Fock equation,

which formally reads

$$\int d\mathbf{r}' h(\mathbf{r}, \mathbf{r}') \varphi(\mathbf{r}') = \varepsilon \varphi(\mathbf{r}), \quad (7)$$

where the Lagrangian multiplier ε is the single-particle energy including the rest mass of the nucleon. The single-particle Hamiltonian $h(\mathbf{r}, \mathbf{r}')$ contains the kinetic energy h^K , the direct local potential h^D , and the exchange non-local potential h^E ,

$$h^K(\mathbf{r}, \mathbf{r}') = [\boldsymbol{\alpha} \cdot \mathbf{p} + \beta M] \delta(\mathbf{r}, \mathbf{r}'), \quad (8a)$$

$$h^D(\mathbf{r}, \mathbf{r}') = [\Sigma_T(\mathbf{r}) \gamma_5 + \Sigma_0(\mathbf{r}) + \beta \Sigma_S(\mathbf{r})] \delta(\mathbf{r}, \mathbf{r}'), \quad (8b)$$

$$h^E(\mathbf{r}, \mathbf{r}') = \begin{pmatrix} Y_G(\mathbf{r}, \mathbf{r}') & Y_F(\mathbf{r}, \mathbf{r}') \\ X_G(\mathbf{r}, \mathbf{r}') & X_F(\mathbf{r}, \mathbf{r}') \end{pmatrix}. \quad (8c)$$

The tensor force contributes only to the nonlocal self-energies X_G , X_F , Y_G , and Y_F . See Refs. [74, 77, 89] for

TABLE I. Expressions for \mathcal{F}_ϕ in Eq. (10) for each meson-nucleon coupling. M^* is the Dirac mass of nucleons.

ϕ	\mathcal{F}_ϕ	ϕ	\mathcal{F}_ϕ
ω -V	$\frac{g_\omega(1)g_\omega(2)}{4M^*(1)M^*(2)}$	π -PV	$-\frac{f_\pi(1)f_\pi(2)}{m_\pi^2}$
ρ -V	$\frac{g_\rho(1)g_\rho(2)}{4M^*(1)M^*(2)}$	ρ -T	$\frac{f_\rho(1)f_\rho(2)}{4M^2}$
		ρ -VT	$\frac{f_\rho(1)g_\rho(2)}{4MM^*(2)} + (1 \leftrightarrow 2)$

the full expressions of these quantities.

Obviously, the Hartree-Fock equation shall be solved iteratively. For the open-shell nuclei, the pairing correlation are treated using the BCS method. The zero-range density-dependent interaction [90],

$$V(r_1, r_2) = V_0 \delta(r_1 - r_2) \left[1 - \frac{\rho_b(r)}{\rho_{\text{sat}}} \right], \quad (9)$$

is adopted to calculate the pairing matrix elements. The strength V_0 is uniformly chosen as -500 MeV fm^3 . It can be shown that the shell structure and its evolution in the nuclei studied here are not sensitive to the value of V_0 over a wide range [26].

B. Contributions of tensor force

As already mentioned, the tensor force in each meson-nucleon coupling was identified through the nonrelativistic reduction [66]. The method to quantitatively evaluate the contributions of the tensor force was established as well. Here, we will not go into the details of nonrelativistic reduction, but merely show the components of the tensor force in the relevant meson-nucleon couplings in a uniformed expression as

$$\hat{\mathcal{V}}_\phi^t = \frac{1}{m_\phi^2 + q^2} \mathcal{F}_\phi S_{12}, \quad (10)$$

where S_{12} is the operator of the tensor force in the momentum space, which reads

$$S_{12} \equiv (\boldsymbol{\sigma}_1 \cdot \mathbf{q})(\boldsymbol{\sigma}_2 \cdot \mathbf{q}) - \frac{1}{3}(\boldsymbol{\sigma}_1 \cdot \boldsymbol{\sigma}_2)q^2. \quad (11)$$

The coefficient \mathcal{F}_ϕ associated with a given meson-nucleon coupling reflects the sign and the rough strength of the tensor force, as displayed in Table I.

To evaluate quantitatively the contributions of the tensor force $\hat{\mathcal{V}}_\phi^t$ in each meson-nucleon coupling, one first needs to calculate its contributions to the two-body interaction matrix elements. The explicit formulas are referred to the Appendix C in Ref. [66]. Further, one can calculate the contributions of the tensor force to the non-local self-energies, and eventually its contributions to the single-particle energies.

III. RESULTS AND DISCUSSION

A. $N = 82$ isotones

First, we study the evolution of the energy difference between the states $\nu 1i_{13/2}$ and $\nu 1h_{9/2}$, i.e., $\Delta\varepsilon \equiv \varepsilon_{\nu 1i_{13/2}} - \varepsilon_{\nu 1h_{9/2}}$, along the $N = 82$ isotones. Shown in Fig. 1 are the energy differences as functions of the proton number Z , normalized with respect to the values at $Z = 58$. In Fig. 1(a), one can see that the original experimental data taken from Ref. [50] present a distinct kink at $Z = 64$. Since the experimental data of single-particle energies contain the beyond-mean-field correlation, they are not supposed to compare directly with the corresponding calculated results based on the pure mean-field approximation, as emphasized by a series of studies [25, 26, 34, 49, 51, 91]. However, to our knowledge, there is still no accessible RHF + PVC calculation. On the other hand, we notice that the quasiparticle PVC (QPVC) calculation based on the RMF theory using the nonlinear effective interaction NL3* was performed for the $N = 82$ isotones [49]. It was also suggested that the effective tensor force has to be quenched as compared with the earlier estimates without considering the PVC effects [49]. Therefore, here we extract the difference between the results of RMF and QPVC, and deem it, to some extent, the accurate PVC effects. By excluding the PVC effects from the original data [50], we get the corresponding “pseudo-data”, which are denoted by the open squares in Fig. 1(a). The “pseudo-data” also present a distinct kink, but the turning point is shifted to $Z = 58$. Despite the change of the turning point, the slope of the original data is remarkably changed by the PVC effects only in the region between $Z = 58$ and $Z = 64$, while it remains almost unchanged in the other regions.

The calculated results by the RHF theory using the density-dependent effective interactions PKA1 and PKO*i* ($i = 1, 2, 3$) are displayed in Fig. 1(a). It can be found that the energy differences calculated by PKO1 and PKO3 present distinct kinks at $Z = 58$, which is in consistence with the “pseudo-data”. In contrast, PKA1 gives a very small kink, and PKO2 presents an approximately linearly increasing trend.

Using the method developed in Ref. [66], we calculate the contributions of the tensor force to the single-particle energies. We then exclude the tensor-force contributions from the results of the full calculation. The results, where the contributions of the tensor force have been subtracted, are shown in Fig. 1(b). One can see that all the RHF effective interactions give almost identical results after excluding the tensor force. This indicates that the differences in the results by different effective interactions mainly arise from the tensor forces. In addition, the results without the tensor force present an approximately linearly increasing trend. This shows the crucial role of the tensor force on the evolution of the single-particle energy differences.

In Ref. [66], it is shown that the tensor force arising

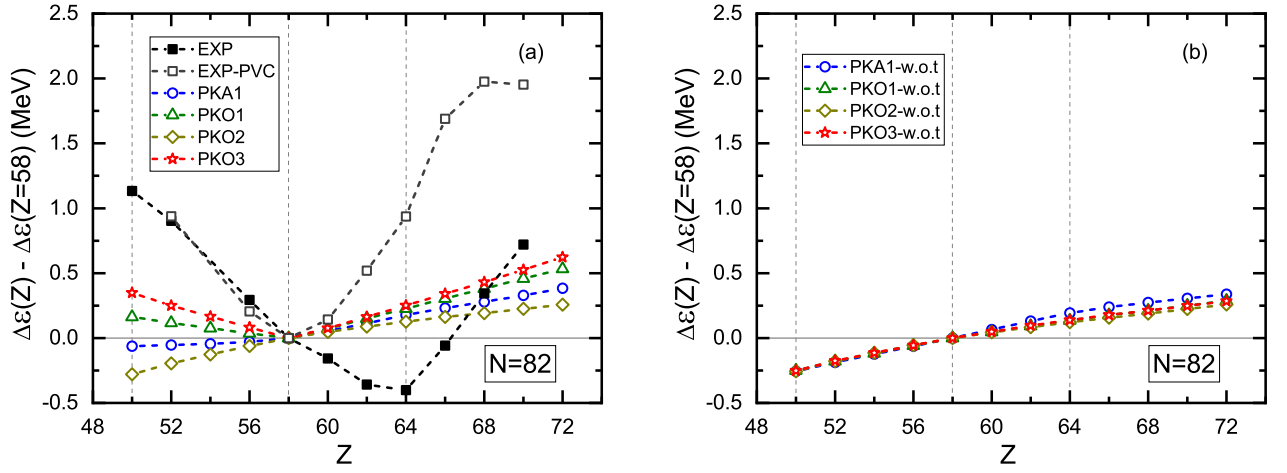


FIG. 1. Energy differences $\Delta\epsilon \equiv \epsilon_{\nu 1i_{13/2}} - \epsilon_{\nu 1h_{9/2}}$ in the $N = 82$ isotones as functions of the proton number. Panel (a) shows the calculated results by the RHF theory with the effective interactions PKA1 and PKO i ($i = 1, 2, 3$). Panel (b) shows the results of the same calculations but without the tensor-force contributions. The pairing is treated with the BCS method. The experimental data for comparison include the original ones (filled squares) from Ref. [50] as well as the ones (open squares) in which the correlation of particle-vibration coupling [49] is subtracted. All the experimental data and the calculated results are normalized with respect to their corresponding values at $Z = 58$. See the text for details.

from the π -PV coupling dominates over those from all other nucleon-meson couplings. This is true not only for PKA1 but also for PKO1 and PKO3. As shown in Eq. (4), the π -PV coupling strength in the effective interactions adopted here depends on the baryon density exponentially. Its value at zero density, i.e., $f_\pi(0)$, in PKO3 is the same with that in PKO1, but the factor of density dependence a_π in PKO3 is smaller [26]. Therefore, the tensor force in PKO3 is stronger than that in PKO1. In PKA1, the contribution of the tensor force from the ρ -T coupling, which is not considered in the PKO series, remarkably cancels that from the π -PV one [66]. As a consequence, the net tensor-force effect in PKA1 is weaker than those in both PKO1 and PKO3. Notice that the π -PV coupling is not included in PKO2 at all. According to the discussion above, one can recognize that, for the strength of the tensor force, $\text{PKO3} > \text{PKO1} > \text{PKA1} > \text{PKO2}$. Keeping this conclusion in mind, let us turn back to Fig. 1 again. Among all the RHF effective interactions, PKO3 reproduces the data best, even though it is still quite far away from perfect. While it is not as good as PKO3, PKO1 is much better than PKA1 and PKO2. Considering the relative strengths of the tensor forces in these RHF effective interactions, one can conclude that the effective interaction with stronger tensor force reproduces the evolution of the single-particle energy difference better. Further, it implies that the tensor force in the current RHF effective interactions seems in general too weak, and stronger tensor force is appealing for the future development of the effective interactions.

Next, we will discuss explicitly the effects of the tensor force on the evolution of the energy difference between the states $\nu 1i_{13/2}$ and $\nu 1h_{9/2}$ along the $N = 82$ isotones.

The contributions of the tensor force to the energy differences, calculated with the effective interactions PKA1 and the PKO series, are shown in the different panels of Fig. 2.

For the results of PKA1, shown in Fig. 2(a), the net contribution of the tensor forces of all the involved nucleon-meson couplings has a flat minimum around $Z = 64$, which is at same position of the minimum of the original experimental data. As expected, the tensor force from the π -PV coupling is the most remarkable compared with those from the other couplings, and it also gives a minimum around $Z = 64$. Actually, the trend of the net contribution of the tensor forces is mainly determined by the tensor force from the π -PV coupling. Meanwhile, one can see that the contribution of the tensor force from the π -PV coupling is partially cancelled by those from the other couplings, especially the ρ -T and ρ -VT ones. It is also worth noticing that the tensor-force contribution from the ω -V coupling is not always opposite to that from the π -PV one. This seems in conflict with the fact that the sign of the tensor force from ω -V coupling is opposite to that from π -PV one, as shown in Table I. In fact, it is not a conflict. The reason is that the ω -V coupling does not contribute to the proton-neutron interaction and its tensor-force contribution comes only from the neutron-neutron interaction. With the increasing of the proton number, the wave functions of the neutron states change as well, which consequently gives rise to the changes of the tensor-force contribution from the ω -V coupling. Hence, the properties of the tensor force from the ω -V coupling presented here, especially its sign, are accidental to some extent.

From Figs. 2(b) and 2(d), it can be seen that the net contributions of the tensor force calculated by PKO1 and

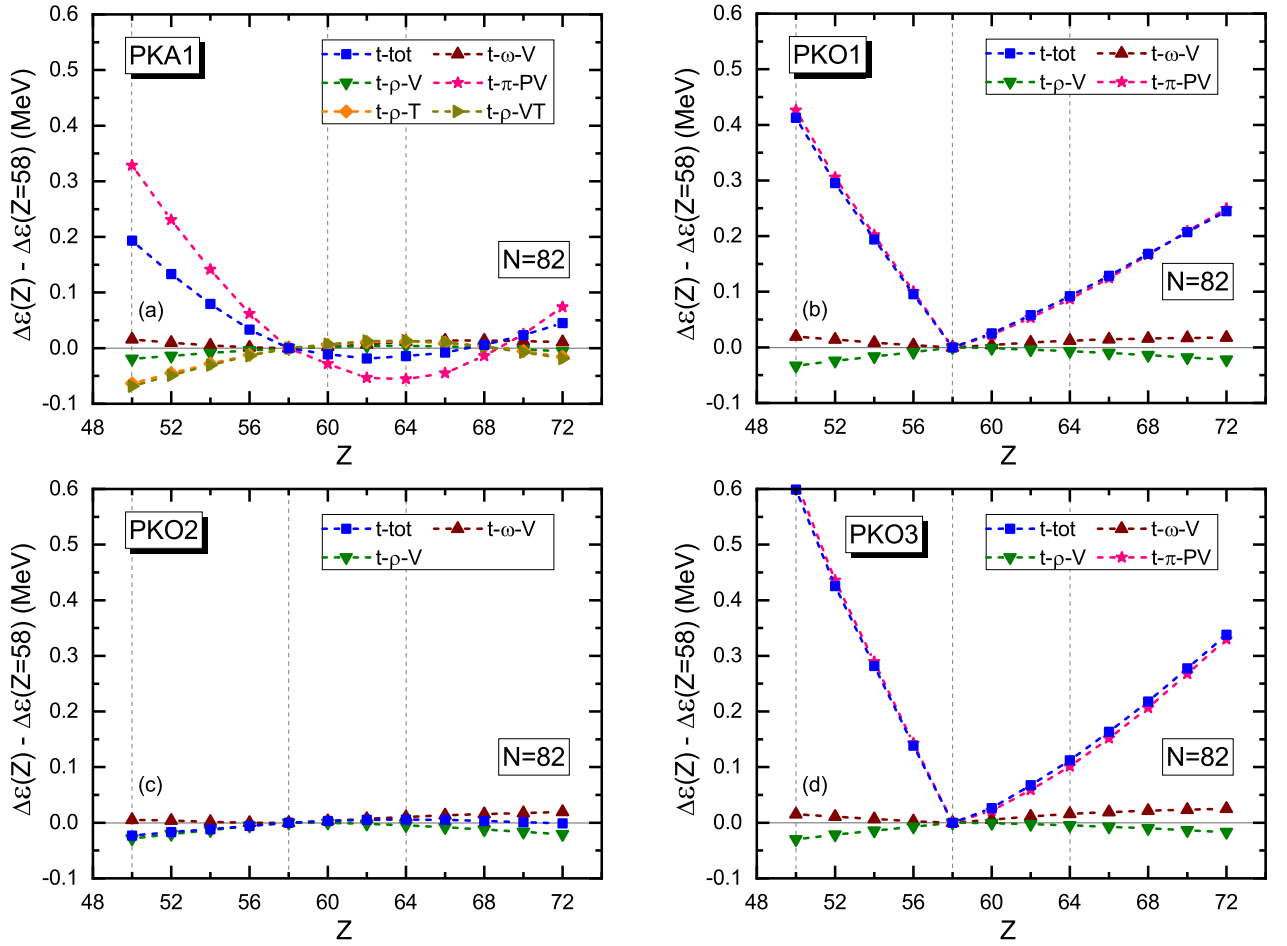


FIG. 2. The tensor-force contributions to the energy differences $\Delta\epsilon \equiv \epsilon_{\nu 1i_{13/2}} - \epsilon_{\nu 1h_{9/2}}$ in the $N = 82$ isotones as functions of the proton number, calculated by the RHF theory with the effective interactions PKA1 and PKO*i* ($i = 1, 2, 3$). The blue filled squares denote the total contributions of the tensor force, while the contributions of the individual coupling are denoted by the other symbols. All the results are normalized with respect to their corresponding values at $Z = 58$.

PKO3 present quite sharp turnings at $Z = 58$, which is exactly the turning point of the “pseudo-data”. Based on the comparison of the results with and without the tensor force displayed in Fig. 1, one can conclude that the reason why PKO1 and PKO3 can present distinct kinks at $Z = 58$ is largely related to the sharp turning of the contribution of tensor force. Moreover, it is noticeable that the net tensor-force contributions in both PKO1 and PKO3 are almost fully determined by the contribution of the π -PV coupling. This is because the tensor force from the ω -V coupling largely cancels that from the ρ -V one. Here, we remind again that the effects of the tensor force from the ω -V coupling are due to the neutron-neutron rather than the proton-neutron interactions. Such a cancellation does not appear for PKA1, mainly due to the considerable contributions of the tensor force from ρ -T coupling as well as the ρ -VT one. In addition, one finds that the contribution of the tensor force in PKO3 is larger than that in PKO1. This results from the fact that the

coupling strength of π -PV coupling in PKO3 is larger, as mentioned above. The results of PKO2 are very different. Because of the absence of both π -PV and ρ -T couplings [26], the proton-neutron tensor force in PKO2 is very weak. Therefore, the net contribution of the tensor force in PKO2 is almost negligible for the shell-structure evolution discussed here, as can be seen from Fig. 2(c).

B. $Z = 50$ isotopes

Figure 3 displays the energy differences between single-particle states $\pi 1h_{11/2}$ and $\pi 1g_{7/2}$ in the $Z = 50$ (Sn) isotopes as functions of the neutron number. Similar with the case of the $N = 82$ isotones studied above, Fig. 3(a) displays both the original experimental data and the “pseudo-data”, where the latter are obtained in the same way as those in the $N = 82$ isotones. The calculations are also performed in the same way as those for

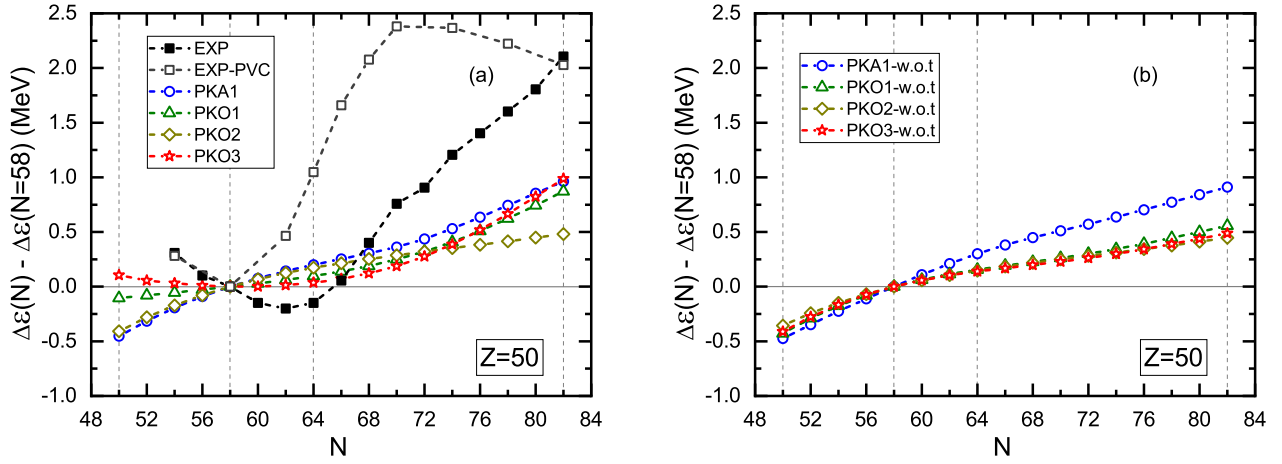


FIG. 3. Similar with Fig. 1, but for the energy differences $\Delta\varepsilon \equiv \varepsilon_{\pi 1h_{11/2}} - \varepsilon_{\pi 1g_{7/2}}$ in the $Z = 50$ isotopes as functions of the neutron number. All the experimental data and the calculated results are normalized with respect to their corresponding values at $N = 58$.

the $N = 82$ isotones. All the experimental data and the calculated results are normalized with respect to their corresponding values at $N = 58$. One can find that the original data presents a minimum at $N = 62$, while it is shifted to $N = 58$ after considering the PVC effects based on RMF. Meanwhile, the PVC effects do not modify remarkably the slope in the region from $N = 54$ to $N = 58$ and that in the region from $N = 64$ to $N = 70$.

Among all the RHF effective interactions used here, only PKO3 gives a visible minimum, which is located around $N = 58$, in consistent with the minimum of the “pseudo-data”. In contrast, the energy differences calculated by all other effective interactions increase monotonically with the neutron number, failing to reproduce the experimental trend even qualitatively. Compared with PKA1 and PKO2, the results of PKO1 are relatively closer to those of PKO3, also closer to the data. Given the relative strengths of the tensor force in these effective interactions, i.e., $\text{PKO3} > \text{PKO1} > \text{PKA1} > \text{PKO2}$, one can suppose again that the tensor force is the main cause of the differences among these results. To make it clearer, we subtract the contributions of the tensor force following what has been done for the $N = 82$ isotones. The results are displayed in Fig. 3(b). Without the contributions of the tensor force, all the RHF effective interactions give similar results, i.e., the energy differences increase monotonically with the neutron number. Thus, the determinant role of the tensor force is confirmed again.

Shown in Fig. 4 are the explicit contributions of the tensor force calculated by PKA1 and PKO series. The net contribution of the tensor force in PKA1, shown in Fig. 4(a), has a minimum around $N = 70$, which is consistent with neither the original data nor the “pseudo-data”. The contribution of the tensor force from the π -PV coupling dominates over those from the other couplings. The net contribution of the tensor force is qualitatively in line with that from the π -PV coupling, and

the former is smaller than the latter in amplitude. This is determined by the relative strengths of the tensor force in each nucleon-meson coupling and the signs of them. The feather is the same as that in the case of $N = 82$ isotones. The details will not be repeated here.

The contributions of the tensor force in PKO1 and PKO3 are shown in Figs. 4(b) and 4(d), respectively. It can be seen that the minima given by PKO1 and PKO3 are both near $N = 64$, which is the same position of the minimum of the original data shown in Fig. 3. As mentioned above, the minimum of the energy differences calculated by PKO3 is near $N = 58$, same as the minimum of the “pseudo-data”. This means the minimum of the contribution of tensor force cannot uniquely determine the minimum of the energy difference. Even though the contributions of the tensor force given by PKO1 and PKO3 are similar with each other, the former fails to reproduce the experimental trend of the shell-structure evolution. Similar with the results for the $N = 82$ isotones, the contribution of the tensor force in PKO3 is larger than that in PKO1, as can be seen in Figs. 4(b) and 4(d). This reminds us that the strength of the tensor force is crucial for reproducing the trend of the experimental data. For PKO2, the contribution of the tensor force is minor due to the absence of the π -PV coupling, as shown in Fig. 4(c).

It is interesting to see the differences between the contributions of the tensor force in the $N = 82$ isotones and those in the $Z = 50$ isotopes, which are especially clear for the results by PKO1 and PKO3. First, for the $Z = 50$ isotopes, there are obvious differences between the net tensor-force contribution and the tensor-force contribution of π -PV coupling. For the $N = 82$ isotones, such a difference is smaller (PKA1) and even invisible (PKO1 and PKO3). The main reason is that the cancellation of the contributions of the tensor force from the ω -V and ρ -V couplings in the $Z = 50$ isotopes is not so enormous

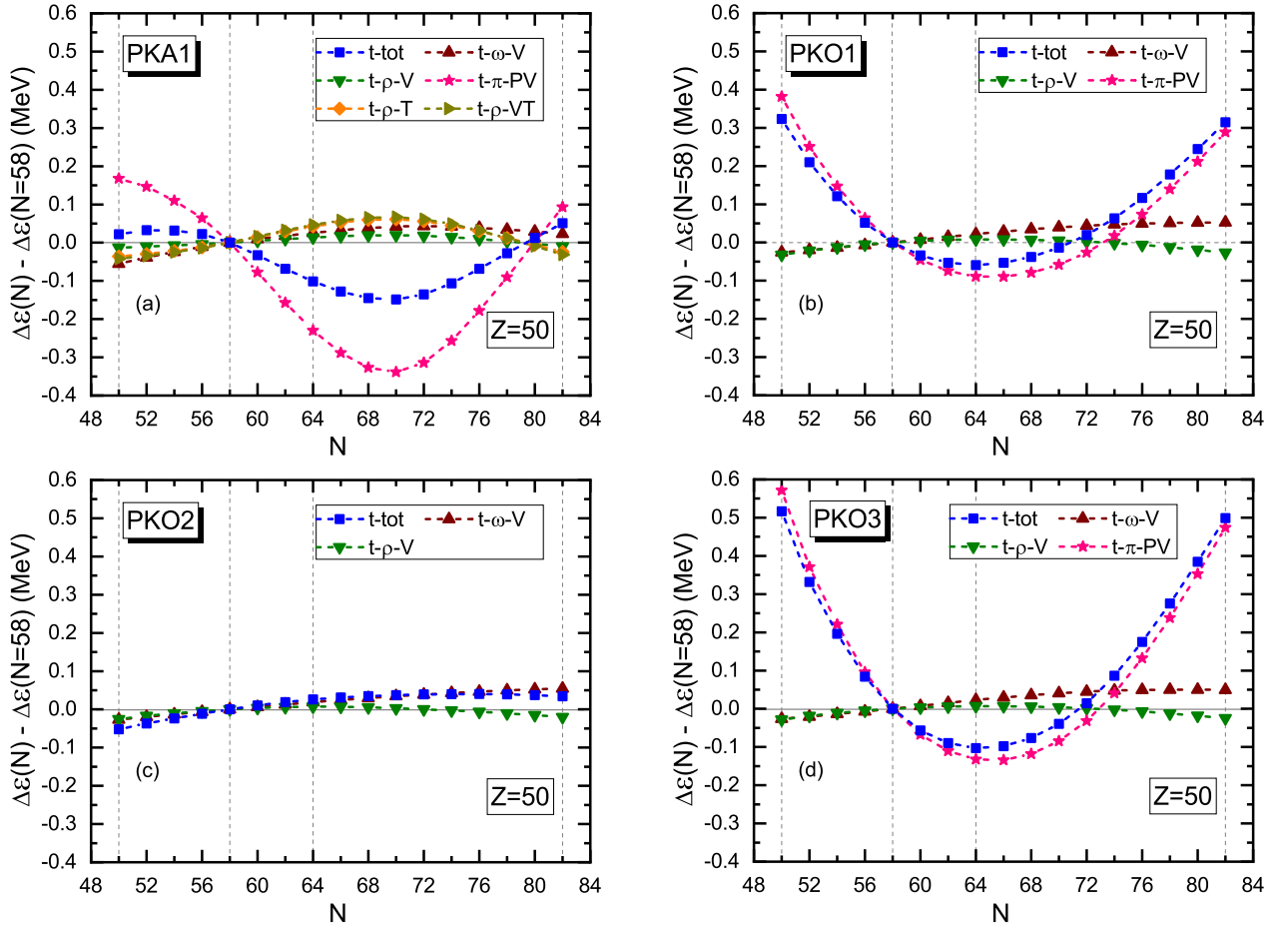


FIG. 4. Similar with Fig. 2, but for the energy differences $\Delta\varepsilon \equiv \varepsilon_{\pi 1h_{11/2}} - \varepsilon_{\pi 1g_{7/2}}$ in the $Z = 50$ isotopes as functions of the neutron number. All the results are normalized with respect to their corresponding values at $N = 58$.

as that in the $N = 82$ isotones. Second, the contribution of the tensor force in the $Z = 50$ isotopes changes very gently around the turning point, while the turning at $Z = 58$ in the $N = 82$ isotones is quite sharp. Such a difference can be understood from the effects of pairing. For the $N = 82$ isotones, since PKO1 and PKO3 give large artificial shells at $Z = 58$, the protons occupy gradually the orbital $\pi 1g_{7/2}$ from $Z = 50$ to $Z = 58$, leaving the orbital $\pi 2d_{5/2}$ almost empty. The orbitals $\pi 1g_{7/2}$ and $\pi 2d_{5/2}$ are spin-down and spin-up, respectively, and their tensor-force effects on the energy differences under discussion here are opposite to each other. It is the sudden change of the occupation of $\pi 2d_{5/2}$ at $Z = 60$ that results in the sharp turning. In contrast, the $N = 58$ shell gaps in the $Z = 50$ isotopes are not so pronounced in the calculations here. Therefore, for the $Z = 50$ isotopes with the neutron numbers from 52 to 64, both the orbitals $\nu 1g_{7/2}$ and $\nu 2d_{5/2}$ have nonvanishing occupation probabilities and their tensor-force effects partially cancels each other. This is the key reason why there is no sharp change around $N = 58$. The properties of the slope around $N, Z = 64$ and 70 , which belong to the critical

subshells, can also be understood by the magnitudes of the relevant gaps and the pairing effects. We will no longer go into the details since the mechanism is similar.

C. Exploration of the strength of tensor force

Based on the discussion above, one finds that the tensor force in the current RHF effective interactions may be too weak to reproduce the evolution of the single-particle energy differences. In fact, such an point of view was declared more than ten years ago [26]. Similar conclusion was also drawn through the analysis of the evolutions of several magical shells [66] and the spin-orbital splittings in the neutron drops [91, 92]. Considering that the π -PV coupling is the most important carrier of the tensor force, it is natural to explore the strength of the tensor force by enlarging the π -PV coupling strength f_π . Through such an investigation, we expect to give some guidance for developing the effective interactions with well constrained tensor forces in the relativistic framework.

Considering the exponential density dependence of f_π ,

as shown in Eq. (4), one can enlarge it in two ways: (i) multiplying a factor λ ($\lambda > 1$) as a whole, or (ii) weakening the density dependence by multiplying a factor η ($\eta < 1$) in the coefficient a_π . Obviously, the later strategy does not change the value at zero density, but make f_π decrease more slowly with the baryon density.

Taking PKO1 as an example, we will investigate how the enhancement of f_π , in the two different ways above, affects the description of the evolution of the energy difference discussed in the previous subsections. First, we multiply f_π by different λ ($\lambda = 1.0, 1.1, 1.2, 1.3, 1.4$, and 1.5), and then calculate the energy differences between the states $\nu 1i_{13/2}$ and $\nu 1h_{9/2}$ in the $N = 82$ isotones and those between the states $\pi 1h_{11/2}$ and $\pi 1g_{7/2}$ in the $Z = 50$ isotopes. In Fig. 5(a), it can be seen that with the enhancing of the π -PV coupling, the results of $N = 82$ isotones change remarkably and approach the data gradually in the region of $Z \leq 58$. Similar properties are found for the $Z = 50$ isotopes in the region of $N \leq 58$. Note that in the region of $N, Z > 58$, the energy differences in both the isotonic and isotopic chains are not sensitive enough to the multiplier λ . In particular, for the $N = 82$ isotones, the energy differences are almost independent to λ when $Z > 58$. It is worth mentioning once more that for the $N = 82$ isotones ($Z = 50$ isotopes) with $Z \leq 58$ and $64 \leq Z \leq 68$ ($N \leq 58$ and $64 \leq N \leq 68$), the original data and the “pseudo-data” present almost the same slopes. Thus, the data in these regions are supposed to be more reliable references for the mean-field calculations. When $\lambda = 1.5$, the data of the $Z = 50$ isotopes with $N \leq 58$ are reproduced quite well. However, for the $N = 82$ isotones with $Z \leq 58$, it seems that one needs to further enlarge the f_π . Nevertheless, this may not work so well as expected. One can see that the trend starts to become flat around $Z = 50$ when $\lambda = 1.5$. This means that when λ is too large, the shell closure at $Z = 50$ breaks down and the pairing correlation arises. Therefore, it is unlikely to reproduce the data better with even larger λ . Meanwhile, larger λ may worsen the description of the $Z = 50$ isotopes with overestimated slope in the region of $N \leq 58$.

Now let us turn to the alternative way to enhance the π -PV coupling, i.e., reducing the coefficient of density dependence a_π . In Fig. 6 are shown the results of PKO1 with $a_\pi \rightarrow \eta a_\pi$ ($\eta = 1.0, 0.8, 0.6, 0.4, 0.2$, and 0.0). One can find that the evolutions of both chains change remarkably with the reduction of a_π over the whole region discussed here. When $\eta \simeq 0.4$, the data in the regions of $N, Z \leq 58$ are reproduced quite well. Moreover, for the $N = 82$ isotones ($Z = 50$ isotopes) with $64 \leq Z$ ($N \leq 68$), reducing a_π can also improve the description, whereas increasing f_π as a whole does not work well.

Based on the discussion above, it is found that enlarging the strength of π -PV coupling properly can significantly improve the description of the evolution of the single-particle energy difference. Compared with increasing f_π with a factor, reducing its density dependence is a preferable way. It should be noted that we did not per-

form a self-consistent fitting. Thus, the optimum values of λ and η given above should not be taken too seriously, but understood qualitatively.

The weak density dependence of f_π is related not only to the strength of the tensor force but also to the in-medium effects on it. It has been argued that the bare tensor force does not undergo significant modification during the renormalization procedure [93, 94]. In other words, the effective tensor force in the nuclear medium would be similar with the bare one. Such a property is known as “renormalization persistency”. In the RHF theory with the density-dependent coupling strengths, the “renormalization persistency” can naturally manifest as a weak density dependence. The preference for the small a_π , which is shown above, provides a support for the “tensor renormalization persistency” within the scheme of DFT.

IV. SUMMARY AND PERSPECTIVES

Within the framework of the RHF theory, the evolutions of the energy difference between the single-neutron states $\nu 1i_{13/2}$ and $\nu 1h_{9/2}$ along the $N = 82$ isotones and that between the single-proton states $\pi 1h_{11/2}$ and $\pi 1g_{7/2}$ along the $Z = 50$ isotopes have been investigated. Our main focus is on the effects of the tensor force. To compare the calculated results with the experimental data as informative as possible, we have adopted not only the original data but also the “pseudo-data” in which the PVC correlation is removed. It is found that the tensor force plays crucial roles in properly describing the shell-structure evolutions. The contributions of the tensor force from each relevant meson-nucleon coupling were studied in details. It is shown that, for PKA1, PKO1, and PKO3, the tensor force from the π -PV coupling plays a decisive role. While for PKO2, which does not explicitly contain the π -PV coupling, the net contribution of the tensor force is not considerable, since the isoscalar ω -V coupling does not contribute to the neutron-proton interaction. By comparing with the data, we find that the strength of the tensor force is of vital importance for reproducing the trend of the data.

In addition, the strength of the tensor force in the CDFT has been further explored. It is found that moderately increasing the coupling strength of π -PV coupling, which eventually enhances the tensor force in the effective interaction, will significantly improve the description of the shell-structure evolution. A systematic comparison shows that weakening the density dependence of the π -PV coupling is a more efficient way than enlarging it with a factor. Our study thus provides a support for the idea of “tensor renormalization persistency” [93, 94], which emphasizes the resemblance between the in-medium effective tensor force and the bare one.

It should be noted that the PVC correlation considered in this work is taken from the calculations based on the RMF theory [49]. Such a treatment is in principle not

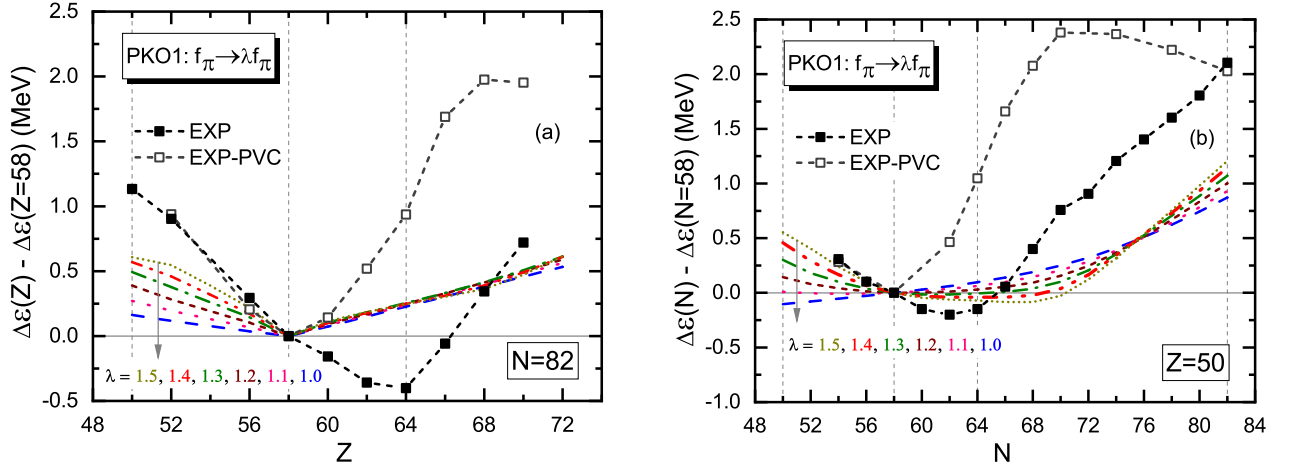


FIG. 5. (a): Energy differences $\Delta\varepsilon \equiv \varepsilon_{\nu 1i_{13/2}} - \varepsilon_{\nu 1h_{9/2}}$ in the $N = 82$ isotones as functions of the proton number, normalized with respect to the values at $Z = 58$. (b): Energy differences $\Delta\varepsilon \equiv \varepsilon_{\pi 1h_{11/2}} - \varepsilon_{\pi 1g_{7/2}}$ in the $Z = 50$ isotopes as functions of the neutron number, normalized with respect to the values at $N = 58$. The calculation is performed by the RHF theory with the effective interaction PKO1, but the π -PV coupling is enlarged by multiplying a factor λ , i.e., $f_{\pi} \rightarrow \lambda f_{\pi}$ ($\lambda = 1.0, 1.1, 1.2, 1.3, 1.4$, and 1.5). For comparison, the experimental data are also given, which are the same as those in Figs. 1 and 3.

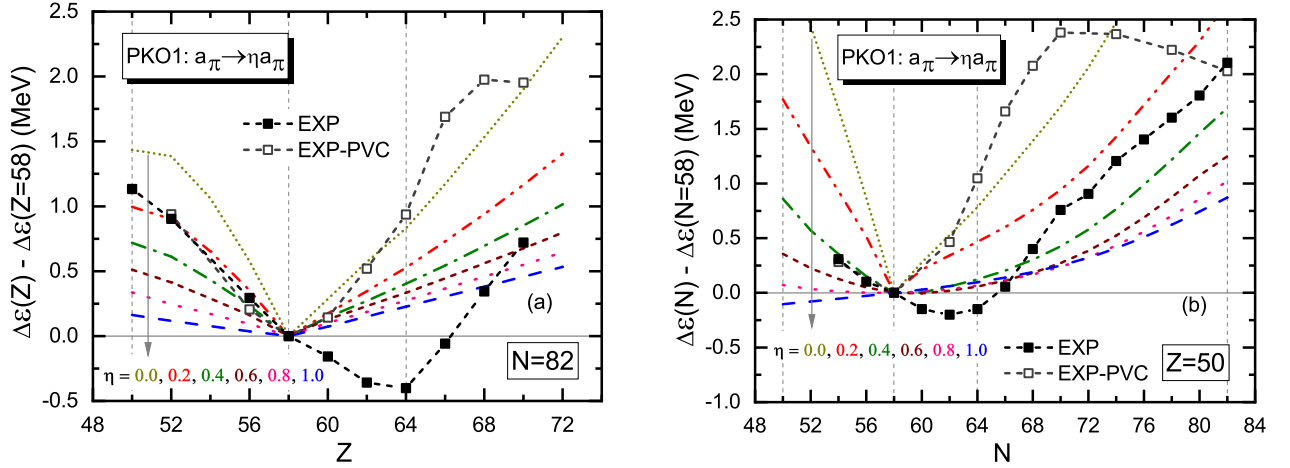


FIG. 6. Similar with Fig. 5, but with $a_{\pi} \rightarrow \eta a_{\pi}$ ($\eta = 1.0, 0.8, 0.6, 0.4, 0.2$, and 0.0).

self-consistent. Thus, as a perspective, we shall take use of the PVC correlation based on the RHF theory, which is expected to be established in the near future. To avoid the distraction of the dynamical correlation, an alternative way is to seek for the meta-data which belong to the pure mean-field level. The spin-orbital splitting calculated by the relativistic Brueckner-Hartree-Fock theory [92, 95, 96] has attracted great attentions [37, 91, 97–100]. Work in this direction is also in progress.

ACKNOWLEDGMENTS

This work is partly supported by the Natural Science Foundation of China under Grant Nos. 11905088, 11675065, and 12075104, and the MOST “Introduction Plan Program of High-Level Foreign Talents” under Grant No. G20200028008, and the JSPS Grant-in-Aid for Early-Career Scientists under Grant No. 18K13549, the JSPS Grant-in-Aid for JSPS Fellows under Grant No. 19J20543, and the JSPS Grant-in-Aid for Scientific Research (S) under Grant No. 20H05648. Z.W. acknowledges the scholarship of China Scholarship Council. T.N. and H.L. thank the RIKEN iTHEMS program and the RIKEN Pioneering Project: Evolution of Matter in the Universe.

-
- [1] O. Haxel, J. H. D. Jensen, and H. E. Suess, *Phys. Rev.* **75**, 1766 (1949).
- [2] M. G. Mayer, *Phys. Rev.* **75**, 1969 (1949).
- [3] I. Tanihata, H. Hamagaki, O. Hashimoto, S. Nagamiya, Y. Shida, N. Yoshikawa, O. Yamakawa, K. Sugimoto, T. Kobayashi, D. Greiner, N. Takahashi, and Y. Nojiri, *Phys. Lett. B* **160**, 380 (1985).
- [4] I. Tanihata, H. Hamagaki, O. Hashimoto, Y. Shida, N. Yoshikawa, K. Sugimoto, O. Yamakawa, T. Kobayashi, and N. Takahashi, *Phys. Rev. Lett.* **55**, 2676 (1985).
- [5] A. Gade and T. Glasmacher, *Prog. Part. Nucl. Phys.* **60**, 161 (2008).
- [6] M. Pfützner, M. Karny, L. V. Grigorenko, and K. Rissager, *Rev. Mod. Phys.* **84**, 567 (2012).
- [7] I. Tanihata, H. Savajols, and R. Kanungo, *Prog. Part. Nucl. Phys.* **68**, 215 (2013).
- [8] P. Campbell, I. Moore, and M. Pearson, *Prog. Part. Nucl. Phys.* **86**, 127 (2016).
- [9] T. Wakasa, K. Ogata, and T. Noro, *Prog. Part. Nucl. Phys.* **96**, 32 (2017).
- [10] T. Nakamura, H. Sakurai, and H. Watanabe, *Prog. Part. Nucl. Phys.* **97**, 53 (2017).
- [11] M. Thoennessen, *Rep. Prog. Phys.* **76**, 056301 (2013).
- [12] M. Wang, G. Audi, F. G. Kondev, W. J. Huang, S. Naimi, and X. Xu, *Chin. Phys. C* **41**, 030003 (2017).
- [13] O. Sorlin and M. G. Porquet, *Prog. Part. Nucl. Phys.* **61**, 602 (2008).
- [14] T. Otsuka, A. Gade, O. Sorlin, T. Suzuki, and Y. Utsuno, *Rev. Mod. Phys.* **92**, 015002 (2020).
- [15] T. Otsuka, R. Fujimoto, Y. Utsuno, B. A. Brown, M. Honma, and T. Mizusaki, *Phys. Rev. Lett.* **87**, 082502 (2001).
- [16] F. Wienholtz *et al.*, *Nature* **498**, 346 (2013).
- [17] D. Steppenbeck *et al.*, *Nature* **502**, 207 (2013).
- [18] W. Rarita and J. Schwinger, *Phys. Rev.* **59**, 556 (1941).
- [19] E. Gerjuoy and J. Schwinger, *Phys. Rev.* **61**, 138 (1942).
- [20] M. Bender, P. H. Heenen, and P. G. Reinhard, *Rev. Mod. Phys.* **75**, 121 (2003).
- [21] T. Otsuka, T. Suzuki, R. Fujimoto, H. Grawe, and Y. Akaishi, *Phys. Rev. Lett.* **95**, 232502 (2005).
- [22] H. Nakada, *Phys. Rev. C* **68**, 014316 (2003).
- [23] T. Otsuka, T. Matsuo, and D. Abe, *Phys. Rev. Lett.* **97**, 162501 (2006).
- [24] D. M. Brink and Fl. Stancu, *Phys. Rev. C* **75**, 064311 (2007).
- [25] T. Lesinski, M. Bender, K. Bennaceur, T. Duguet, and J. Meyer, *Phys. Rev. C* **76**, 014312 (2007).
- [26] W. H. Long, H. Sagawa, J. Meng, and N. Van Giai, *Europhys. Lett.* **82**, 12001 (2008).
- [27] W. Zou, G. Colò, Z. Y. Ma, H. Sagawa, and P. F. Bortignon, *Phys. Rev. C* **77**, 014314 (2008).
- [28] H. Nakada, *Phys. Rev. C* **78**, 054301 (2008).
- [29] M. Moreno-Torres, M. Grasso, H. Z. Liang, V. De Donno, M. Anguiano, and N. Van Giai, *Phys. Rev. C* **81**, 064327 (2010).
- [30] Y. Z. Wang, J. Z. Gu, J. M. Dong, and X. Z. Zhang, *Phys. Rev. C* **83**, 054305 (2011).
- [31] Y. Z. Wang, J. Z. Gu, X. Z. Zhang, and J. M. Dong, *Phys. Rev. C* **84**, 044333 (2011).
- [32] J. M. Dong, W. Zuo, J. Z. Gu, Y. Z. Wang, L. G. Cao, and X. Z. Zhang, *Phys. Rev. C* **84**, 014303 (2011).
- [33] M. Anguiano, M. Grasso, G. Co', V. De Donno, and A. M. Lallena, *Phys. Rev. C* **86**, 054302 (2012).
- [34] H. Sagawa and G. Colò, *Prog. Part. Nucl. Phys.* **76**, 76 (2014).
- [35] H. Z. Liang, J. Meng, and S. G. Zhou, *Phys. Rep.* **570**, 1 (2015).
- [36] Y. Shi, *Phys. Rev. C* **95**, 034307 (2017).
- [37] S. Shen, G. Colò, and X. Roca-Maza, *Phys. Rev. C* **99**, 034322 (2019).
- [38] J. M. Dong and X. L. Shang, *Phys. Rev. C* **101**, 014305 (2020).
- [39] H. Nakada, *Int. J. Mod. Phys. E* **29**, 1930008 (2020).
- [40] B. A. Brown, T. Duguet, T. Otsuka, D. Abe, and T. Suzuki, *Phys. Rev. C* **74**, 061303(R) (2006).
- [41] M. Stanoiu *et al.*, *Phys. Rev. C* **78**, 034315 (2008).
- [42] K. Kaneko, Y. Sun, T. Mizusaki, and M. Hasegawa, *Phys. Rev. C* **83**, 014320 (2011).
- [43] Y. Tsunoda, T. Otsuka, N. Shimizu, M. Honma, and Y. Utsuno, *Phys. Rev. C* **89**, 031301(R) (2014).
- [44] Z. Q. Chen *et al.*, *Phys. Rev. Lett.* **122**, 212502 (2019).
- [45] G. A. Lalazissis, S. Karatzikos, M. Serra, T. Otsuka, and P. Ring, *Phys. Rev. C* **80**, 041301(R) (2009).
- [46] L. G. Cao, G. Colò, H. Sagawa, P. F. Bortignon, and L. Sciacchitano, *Phys. Rev. C* **80**, 064304 (2009).
- [47] C. L. Bai, H. Q. Zhang, H. Sagawa, X. Z. Zhang, G. Colò, and F. R. Xu, *Phys. Rev. C* **83**, 054316 (2011).
- [48] M. Anguiano, G. Co', V. De Donno, and A. M. Lallena, *Phys. Rev. C* **83**, 064306 (2011).
- [49] A. V. Afanasjev and E. Litvinova, *Phys. Rev. C* **92**, 044317 (2015).
- [50] J. P. Schiffer, S. J. Freeman, J. A. Caggiano, C. Deibel, A. Heinz, C. L. Jiang, R. Lewis, A. Parikh, P. D. Parker, K. E. Rehm, S. Sinha, and J. S. Thomas, *Phys. Rev. Lett.* **92**, 162501 (2004).
- [51] G. Colò, H. Sagawa, S. Fracasso, and P. F. Bortignon, *Phys. Lett. B* **646**, 227 (2007).
- [52] M. Zalewski, J. Dobaczewski, W. Satuła, and T. R. Werner, *Phys. Rev. C* **77**, 024316 (2008).
- [53] W. H. Long, N. Van Giai, and J. Meng, *Phys. Lett. B* **640**, 150 (2006).
- [54] W. H. Long, H. Sagawa, N. Van Giai, and J. Meng, *Phys. Rev. C* **76**, 034314 (2007).
- [55] H. Z. Liang, N. Van Giai, and J. Meng, *Phys. Rev. Lett.* **101**, 122502 (2008).
- [56] H. Z. Liang, P. W. Zhao, and J. Meng, *Phys. Rev. C* **85**, 064302 (2012).
- [57] Z. M. Niu, Y. F. Niu, H. Z. Liang, W. H. Long, and J. Meng, *Phys. Rev. C* **95**, 044301 (2017).
- [58] L. J. Wang, J. M. Dong, and W. H. Long, *Phys. Rev. C* **87**, 047301 (2013).
- [59] J. J. Li, W. H. Long, J. Margueron, and N. Van Giai, *Phys. Lett. B* **732**, 169 (2014).
- [60] J. J. Li, J. Margueron, W. H. Long, and N. Van Giai, *Phys. Lett. B* **753**, 97 (2016).
- [61] J. J. Li, W. H. Long, J. L. Song, and Q. Zhao, *Phys. Rev. C* **93**, 054312 (2016).
- [62] J. J. Li, W. H. Long, J. Margueron, and N. Van Giai, *Phys. Lett. B* **788**, 192 (2019).
- [63] L. J. Jiang, S. Yang, J. M. Dong, and W. H. Long, *Phys. Rev. C* **91**, 025802 (2015).

- [64] L. J. Jiang, S. Yang, B. Y. Sun, W. H. Long, and H. Q. Gu, Phys. Rev. C **91**, 034326 (2015).
- [65] Y. Y. Zong and B. Y. Sun, Chin. Phys. C **42**, 024101 (2018).
- [66] Z. Wang, Q. Zhao, H. Liang, and W. H. Long, Phys. Rev. C **98**, 034313 (2018).
- [67] G. F. Bertsch, P. F. Bortignon, and R. A. Broglia, Rev. Mod. Phys. **55**, 287 (1983).
- [68] E. Litvinova and P. Ring, Phys. Rev. C **73**, 044328 (2006).
- [69] E. V. Litvinova and A. V. Afanasjev, Phys. Rev. C **84**, 014305 (2011).
- [70] Y. F. Niu, G. Colò, M. Brenna, P. F. Bortignon, and J. Meng, Phys. Rev. C **85**, 034314 (2012).
- [71] L.-G. Cao, G. Colò, H. Sagawa, and P. F. Bortignon, Phys. Rev. C **89**, 044314 (2014).
- [72] Y. F. Niu, G. Colò, and E. Vigezzi, Phys. Rev. C **90**, 054328 (2014).
- [73] Y. F. Niu, Z. M. Niu, G. Colò, and E. Vigezzi, Phys. Rev. Lett. **114**, 142501 (2015).
- [74] A. Bouyssy, J. F. Mathiot, N. Van Giai, and S. Marcos, Phys. Rev. C **36**, 380 (1987).
- [75] H.-l. Shi, B.-q. Chen, and Z.-y. Ma, Phys. Rev. C **52**, 144 (1995).
- [76] B. Y. Sun, W. H. Long, J. Meng, and U. Lombardo, Phys. Rev. C **78**, 065805 (2008).
- [77] W. H. Long, P. Ring, N. Van Giai, and J. Meng, Phys. Rev. C **81**, 024308 (2010).
- [78] J. P. Ebran, E. Khan, D. Peña Arteaga, and D. Vretenar, Phys. Rev. C **83**, 064323 (2011).
- [79] J. J. Li, W. H. Long, and A. Sedrakian, Eur. Phys. J. A **54**, 133 (2018).
- [80] J. Geng, J. J. Li, W. H. Long, Y. F. Niu, and S. Y. Chang, Phys. Rev. C **100**, 051301(R) (2019).
- [81] J. Geng, J. Xiang, B. Y. Sun, and W. H. Long, Phys. Rev. C **101**, 064302 (2020).
- [82] J. D. Walecka, Ann. Phys. **83**, 491 (1974).
- [83] P. Ring, Prog. Part. Nucl. Phys. **37**, 193 (1996).
- [84] D. Vretenar, A. V. Afanasjev, G. A. Lalazissis, and P. Ring, Phys. Rep. **409**, 101 (2005).
- [85] J. Meng, H. Toki, S. G. Zhou, S. Q. Zhang, W. H. Long, and L. S. Geng, Prog. Part. Nucl. Phys. **57**, 470 (2006).
- [86] T. Nikšić, D. Vretenar, and P. Ring, Prog. Part. Nucl. Phys. **66**, 519 (2011).
- [87] J. Meng and S. G. Zhou, J. Phys. G: Nucl. Part. Phys. **42**, 093101 (2015).
- [88] D. A. Varshalovich, A. N. Moskalev, and V. K. Khersonskii, *Quantum Theory of Angular Momentum* (World Scientific, 1988).
- [89] W. H. Long, *Relativistic Hartree-Fock approach with density-dependent meson-nucleon couplings*, Ph.D. thesis, Peking University, China and Université Paris Sud-Paris XI, France, (2005).
- [90] J. Dobaczewski, W. Nazarewicz, T. R. Werner, J. F. Berger, C. R. Chinn, and J. Dechargé, Phys. Rev. C **53**, 2809 (1996).
- [91] S. H. Shen, H. Z. Liang, J. Meng, P. Ring, and S. Q. Zhang, Phys. Lett. B **778**, 344 (2018).
- [92] S. H. Shen, H. Z. Liang, J. Meng, P. Ring, and S. Q. Zhang, Phys. Rev. C **96**, 014316 (2017).
- [93] T. Otsuka, T. Suzuki, M. Honma, Y. Utsuno, N. Tsunoda, K. Tsukiyama, and M. Hjorth-Jensen, Phys. Rev. Lett. **104**, 012501 (2010).
- [94] N. Tsunoda, T. Otsuka, K. Tsukiyama, and M. Hjorth-Jensen, Phys. Rev. C **84**, 044322 (2011).
- [95] S. H. Shen, J. N. Hu, H. Z. Liang, J. Meng, P. Ring, and S. Q. Zhang, Chin. Phys. Lett. **33**, 102103 (2016).
- [96] S. Shen, H. Liang, W. H. Long, J. Meng, and P. Ring, Prog. Part. Nucl. Phys. **109**, 103713 (2019).
- [97] S. H. Shen, H. Z. Liang, J. Meng, P. Ring, and S. Q. Zhang, Phys. Lett. B **781**, 227 (2018).
- [98] S. Wang, H. Tong, P. Zhao, and J. Meng, Phys. Rev. C **100**, 064319 (2019).
- [99] Q. Zhao, P. Zhao, and J. Meng, Phys. Rev. C **102**, 034322 (2020).
- [100] Y. Ge, Y. Zhang, and J. Hu, Phys. Rev. C **102**, 044304 (2020).